

**Supplementary material for “Direct Observation of the Gas-Phase Criegee Intermediate (CH<sub>2</sub>OO),” by Craig A. Taatjes, Giovanni Meloni, Talitha M. Selby, Adam J. Trevitt, David L. Osborn, Carl J. Percival, Dudley E. Shallcross**

**Experimental Methods**

A slow-flow reactor in which reactions are photolytically initiated is coupled to a photoionization mass spectrometer.<sup>1</sup> The reactions are carried out at 298 K and 4 Torr (530 Pa) pressure. A mixture of (ClCO)<sub>2</sub>, (typical concentrations from  $6 \times 10^{13} \text{ cm}^{-3}$  to  $2 \times 10^{14} \text{ cm}^{-3}$ ), DMSO ( $8 \times 10^{12} \text{ cm}^{-3}$  to  $3 \times 10^{13} \text{ cm}^{-3}$ ), O<sub>2</sub> (up to  $2 \times 10^{16} \text{ cm}^{-3}$ ), and He is flowed through the reactor. Photolysis of (ClCO)<sub>2</sub> at 248 nm yields Cl atoms that react with DMSO to form products including CH<sub>3</sub>S(O)CH<sub>2</sub> radicals that subsequently react with O<sub>2</sub> to form CH<sub>2</sub>OO and other products. The reacting mixture continuously escapes from a pinhole in the reactor and is ionized by tunable synchrotron radiation from the Advanced Light Source at Lawrence Berkeley National Laboratory. The ions are mass-analyzed by a double-focusing mass spectrometer and detected on a time- and position-sensitive detector. The photon energy is scanned yielding time-resolved mass spectra at each photoionization energy. The photon energy and the energy resolution are calibrated by measurement of atomic resonances of Xe and autoionization resonances in O<sub>2</sub>. For each experiment the intensity of all the species (within a mass range of approximately a factor of 8) is recorded as a function of mass-to-charge ratio, reaction time, and photon energy. Average signals taken before the photolysis laser pulse, are subtracted; background-subtracted signal at each photon energy is then normalized for the ionizing photon current.

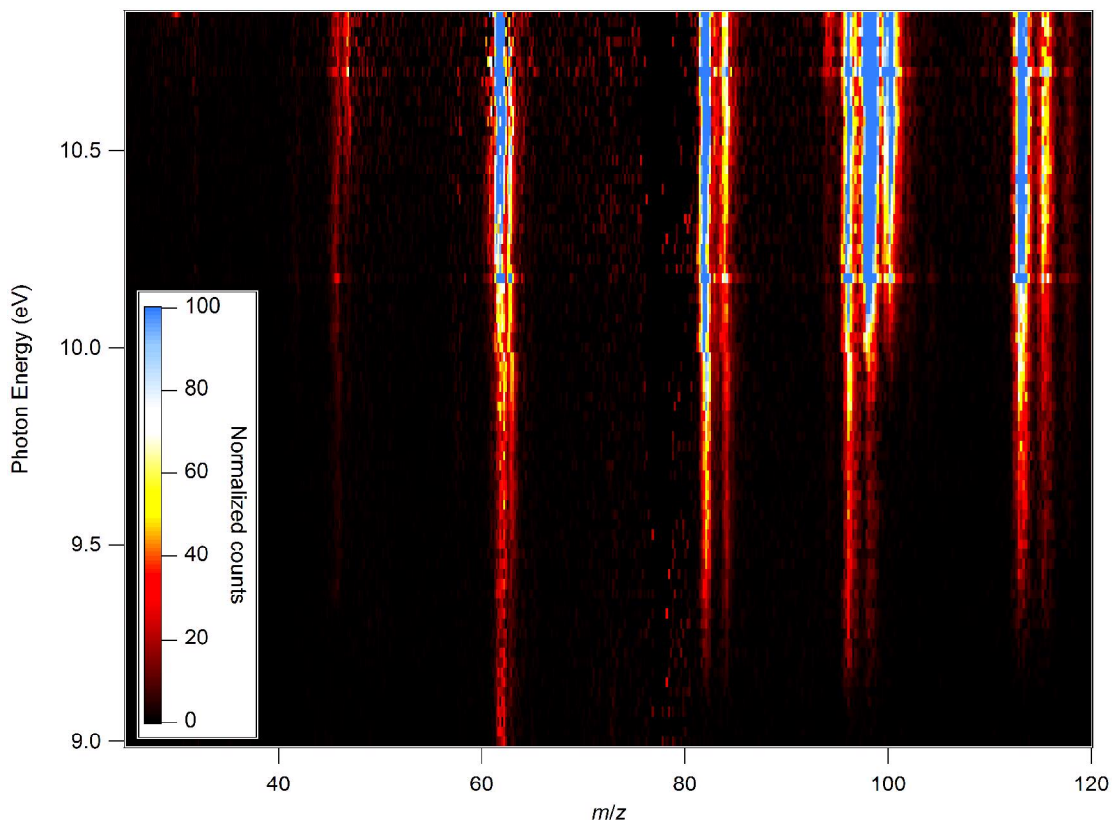


Figure S1. A photoionization efficiency image<sup>2</sup> of species observed in Cl-initiated dimethyl sulfoxide (DMSO) oxidation is shown above. This is the experiment that generated the CH<sub>2</sub>OO spectrum shown in the main paper, with  $\sim 6 \times 10^{12} \text{ cm}^{-3}$  oxalyl chloride,  $\sim 3 \times 10^{13} \text{ cm}^{-3}$  DMSO,  $2 \times 10^{16} \text{ O}_2$ , and the balance He to 530 Pa total pressure. The pre-photolysis signals have been subtracted, so only photolytically-generated species and their reaction products are visible in this image. As no reference spectra are available, the species appearing at  $m/z = 98$  and  $100$  and at  $m/z = 113$  and  $115$  are identified simply on the basis of mass and isotopic ratios as CH<sub>3</sub>S(O)Cl and CH<sub>3</sub>S(O)(Cl)CH<sub>3</sub>, products of Cl addition to DMSO with or without subsequent methyl radical loss. Other prominent species are identified by comparison to literature photoionization efficiency measurements.

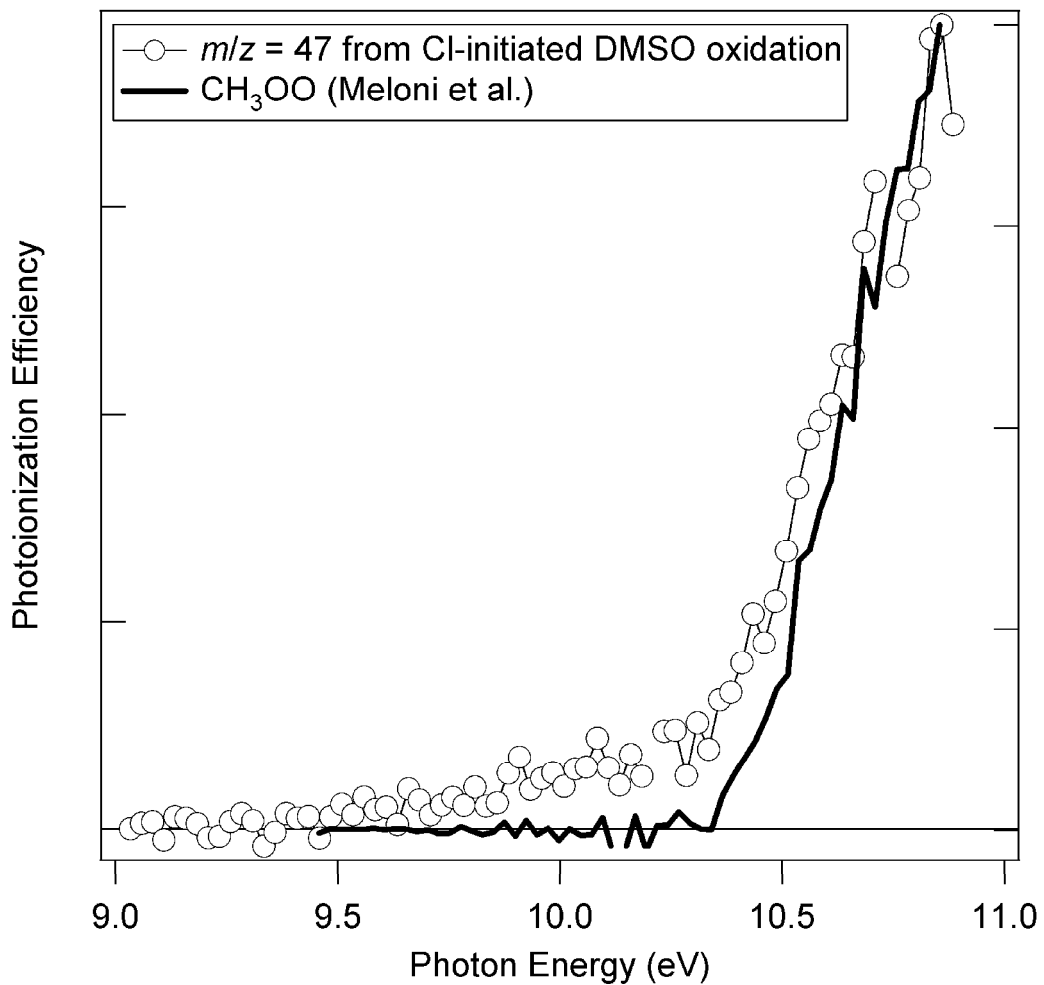


Figure S2. Mass 47 is principally the methyl peroxy radical, CH<sub>3</sub>OO, identified by comparison to the photoionization efficiency reported by Meloni et al.<sup>3</sup>. The contribution at lower photon energies is assigned to the CH<sub>3</sub>S isomer, as no signal is observed below the CH<sub>3</sub>S adiabatic ionization energy of 9.25 eV<sup>4</sup>.

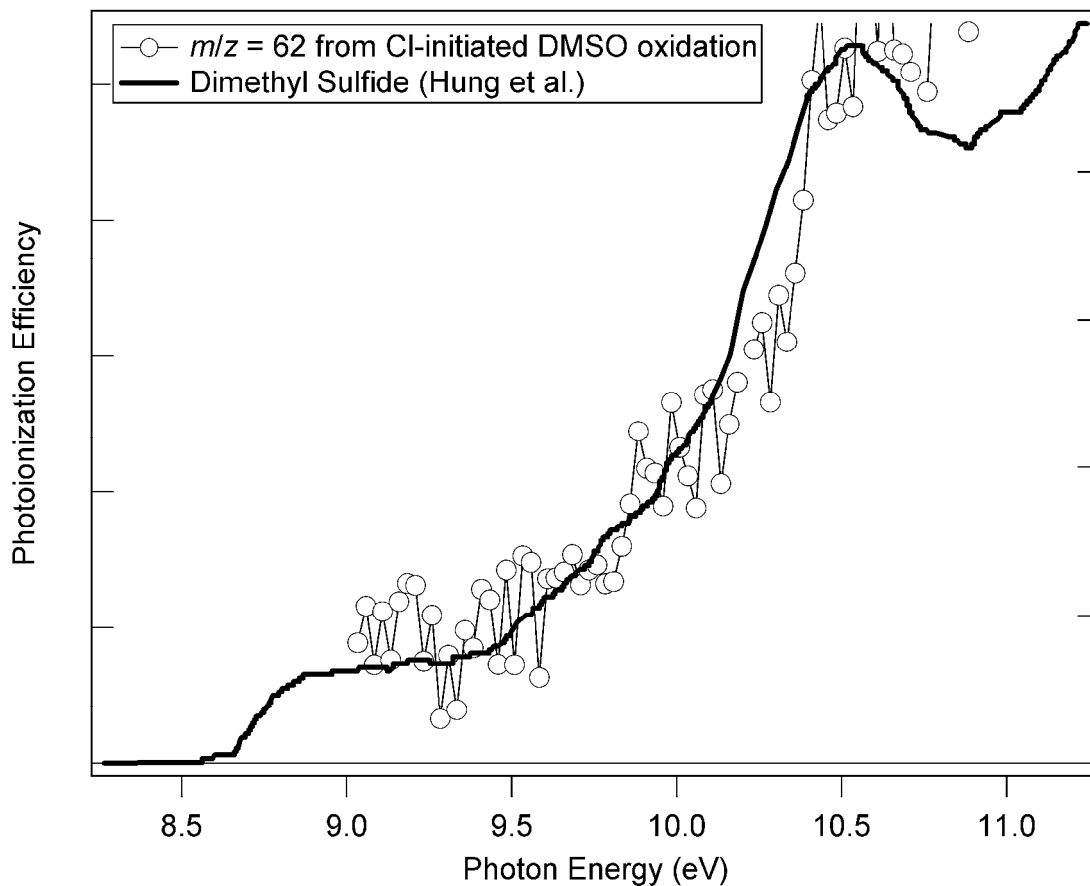


Figure S3. Dimethyl sulfide is observed at  $m/z = 62$ , partially formed by a photolytically-initiated reaction and partially formed by dark reaction of the precursors. The identification is made by comparison to the photoionization spectrum of Hung et al.<sup>5</sup>, shown above.

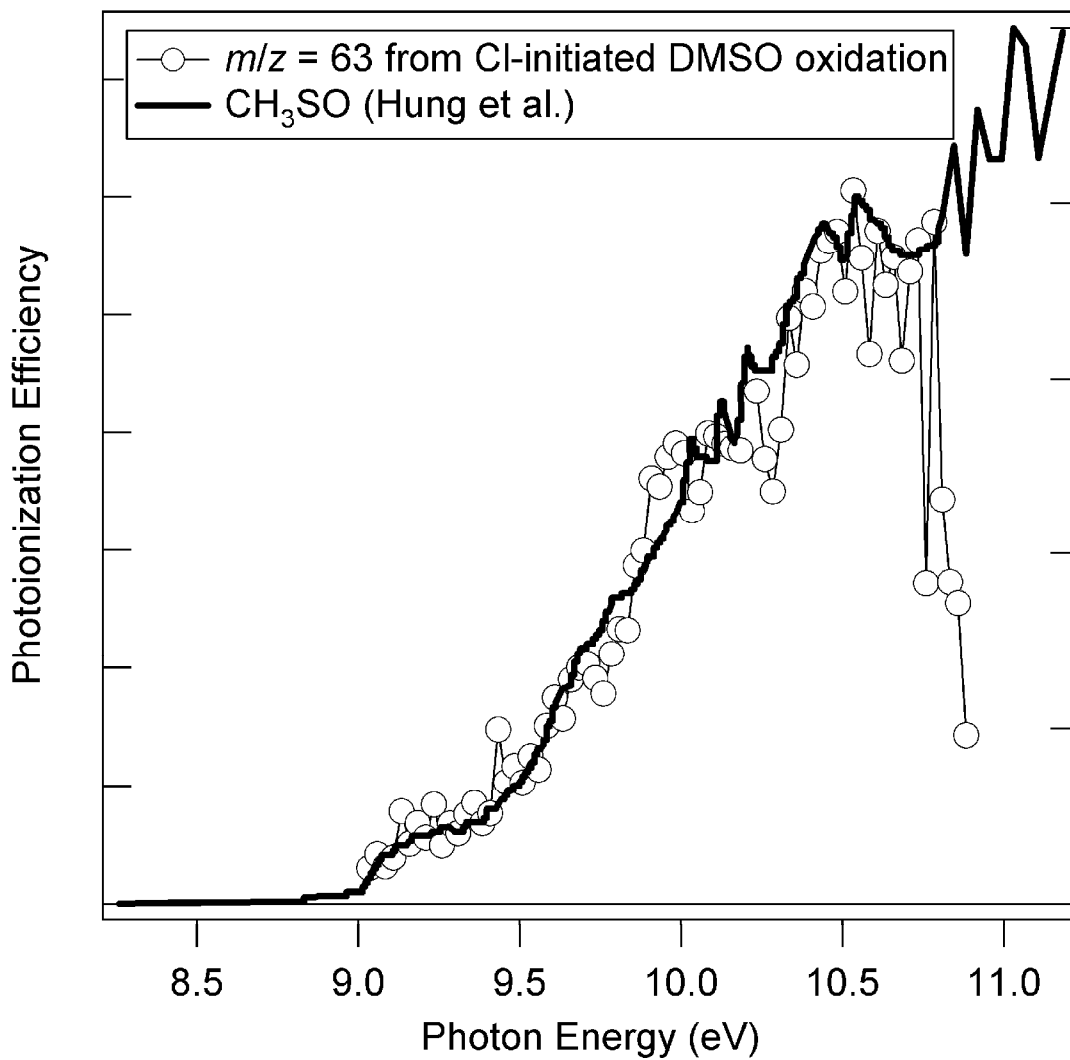


Figure S4. The  $\text{CH}_3\text{SO}$  radical is the co-product of the Criegee intermediate in the reaction of  $\text{CH}_3\text{SOCH}_2$  with  $\text{O}_2$ . The product is identified based on the photoionization spectrum reported by Hung et al.<sup>5</sup>, as shown above.

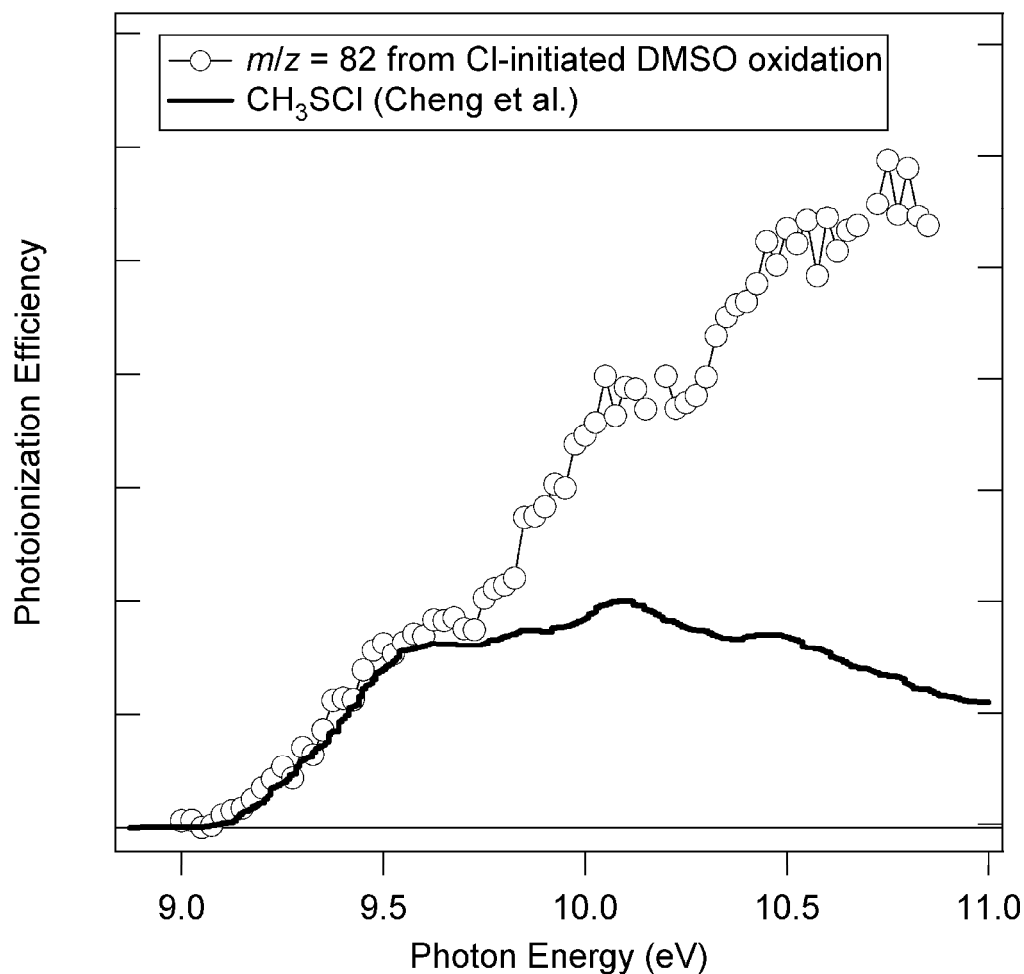


Figure S5. The  $m/z = 82$  and  $m/z = 84$  signals are identified as  $\text{CH}_3\text{SCl}$ , based on the photoionization spectrum of Cheng et al.<sup>6</sup> The features in the Cheng et al. spectrum match well with the present experimental spectrum, but the relative intensities are markedly different. However, a similar discrepancy can be noted between the methyl mercaptan ( $\text{CH}_3\text{SH}$ ) spectrum, reported by Cheng et al.<sup>6</sup> in the same paper, and the spectrum of Nourbakhsh et al.<sup>7</sup>, as shown in Figure S6 below. Scaling the Cheng et al.<sup>6</sup>  $\text{CH}_3\text{SCl}$  spectrum by the same function needed to bring their methyl mercaptan spectrum into agreement with Nourbakhsh et al.<sup>7</sup> also brings their  $\text{CH}_3\text{SCl}$  spectrum into reasonable agreement with the  $m/z = 82$  photoionization efficiency spectrum from Cl-initiated DMSO oxidation.

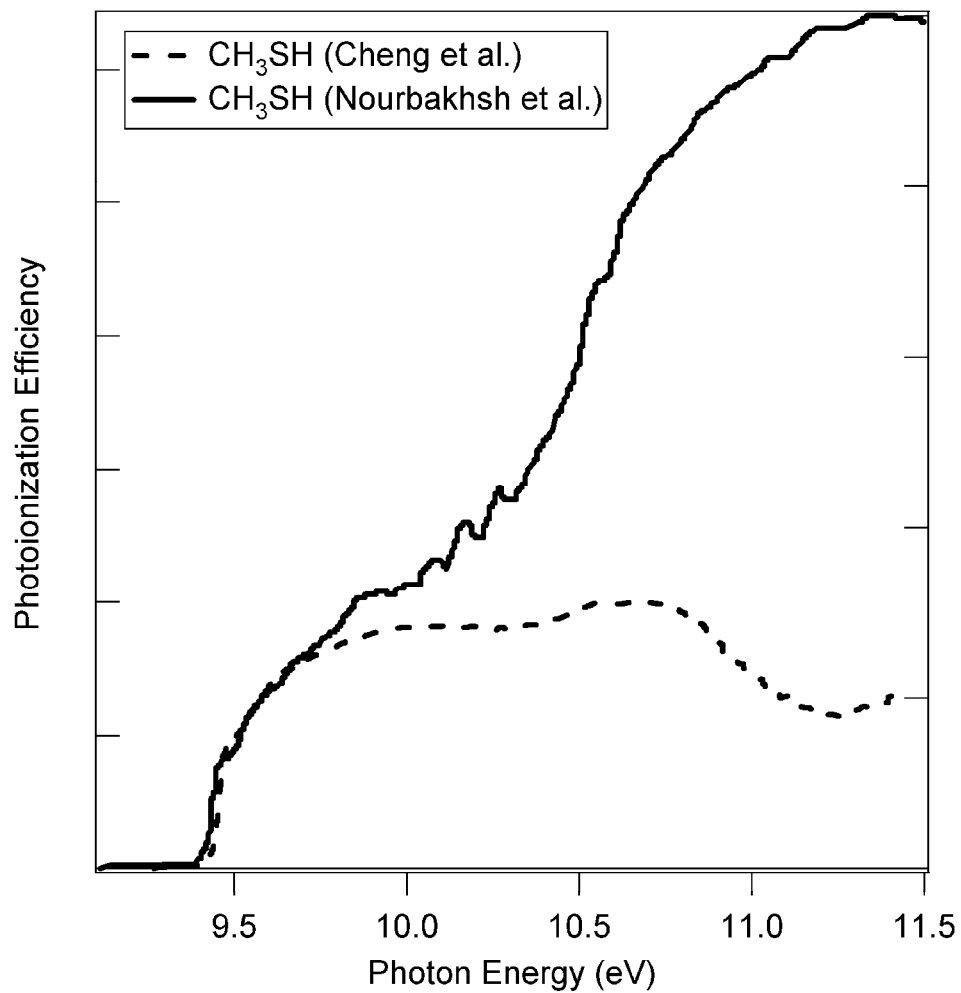


Figure S6. The photoionization spectra of methyl mercaptan reported by Cheng et al.<sup>6</sup> and Nourbakhsh et al.<sup>7</sup>.

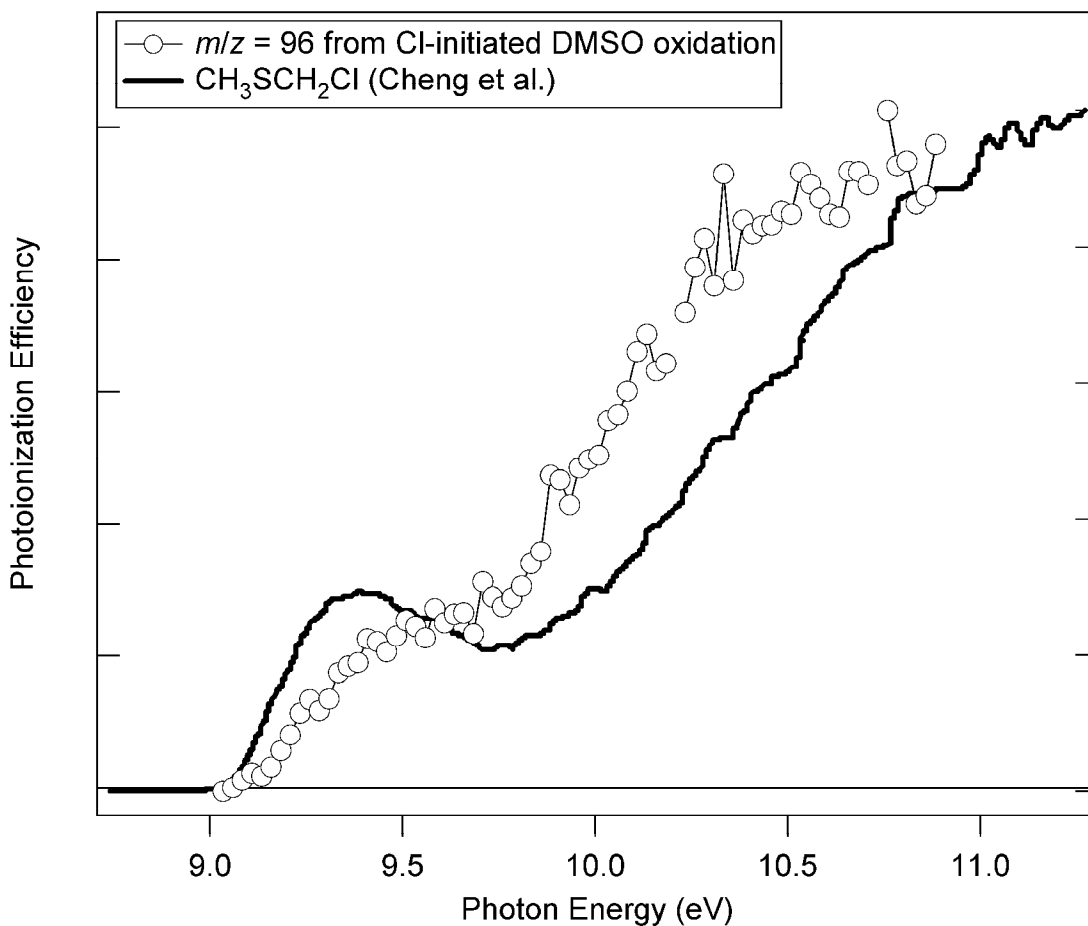


Figure S7. The product at  $m/z = 96$  and  $m/z = 98$  is identified as  $\text{CH}_3\text{SCH}_2\text{Cl}$ . The features observed in the Cheng, Chew, Yu & Yu<sup>8</sup> spectrum are reproduced, but again the relative intensities do not agree. The  $(m/z = 96)/(m/z = 98)$  isotope ratio indicates one Cl atom is present in the species.

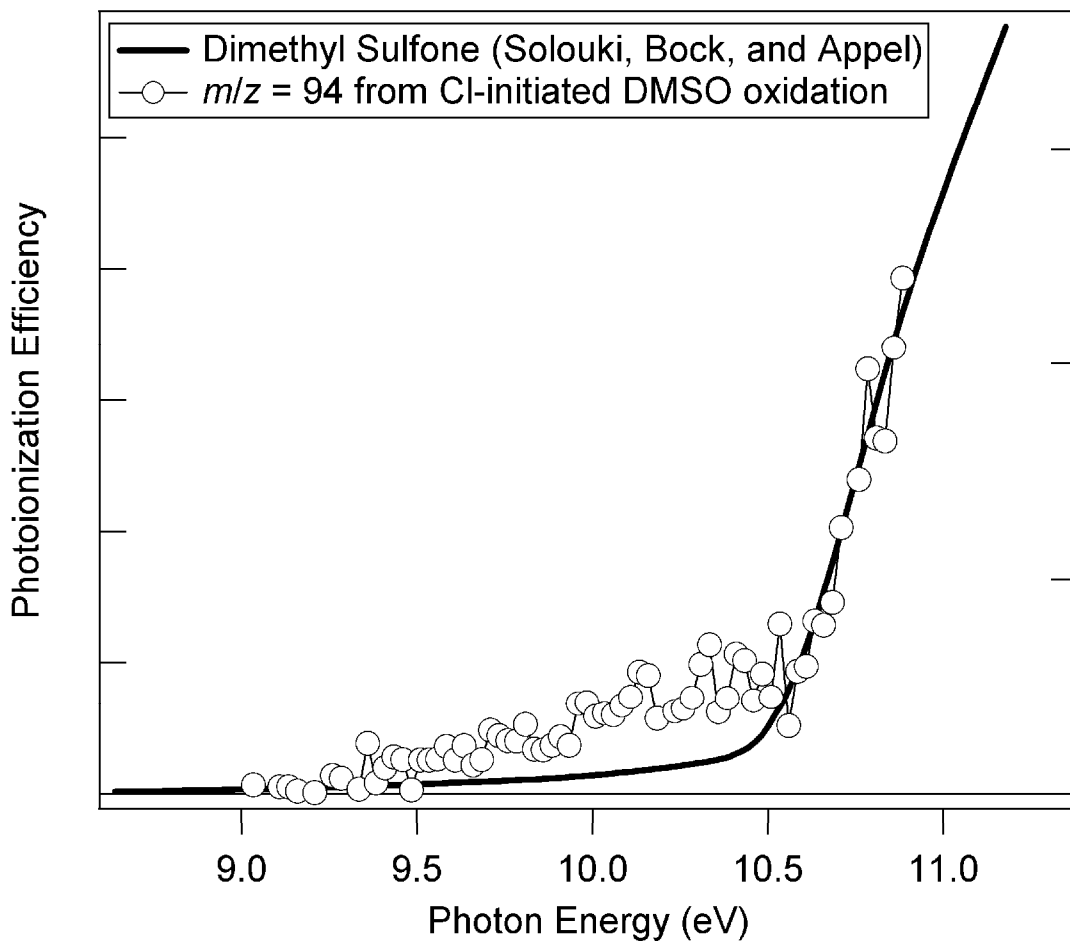


Figure S8. Dimethyl sulfone ( $\text{CH}_3\text{SO}_2\text{CH}_3$ ) is observed at  $m/z = 94$ , as identified from comparison to an integration of the photoelectron spectrum reported by Solouki, Bock, and Appel<sup>9</sup>. The adiabatic ionization energy is calculated (CBS-QB3) to be 10.74 eV; the feature visible to lower ionization energy in the photoelectron spectrum (and more prominently in the photoionization efficiency spectrum above) might arise from ionization of an excited electronic state of dimethyl sulfone. Contributions from dimethyl disulfide ( $\text{CH}_3\text{SSCH}_3$ ) can be ruled out, as its ionization energy is considerably lower (8.18 eV)<sup>10</sup>.

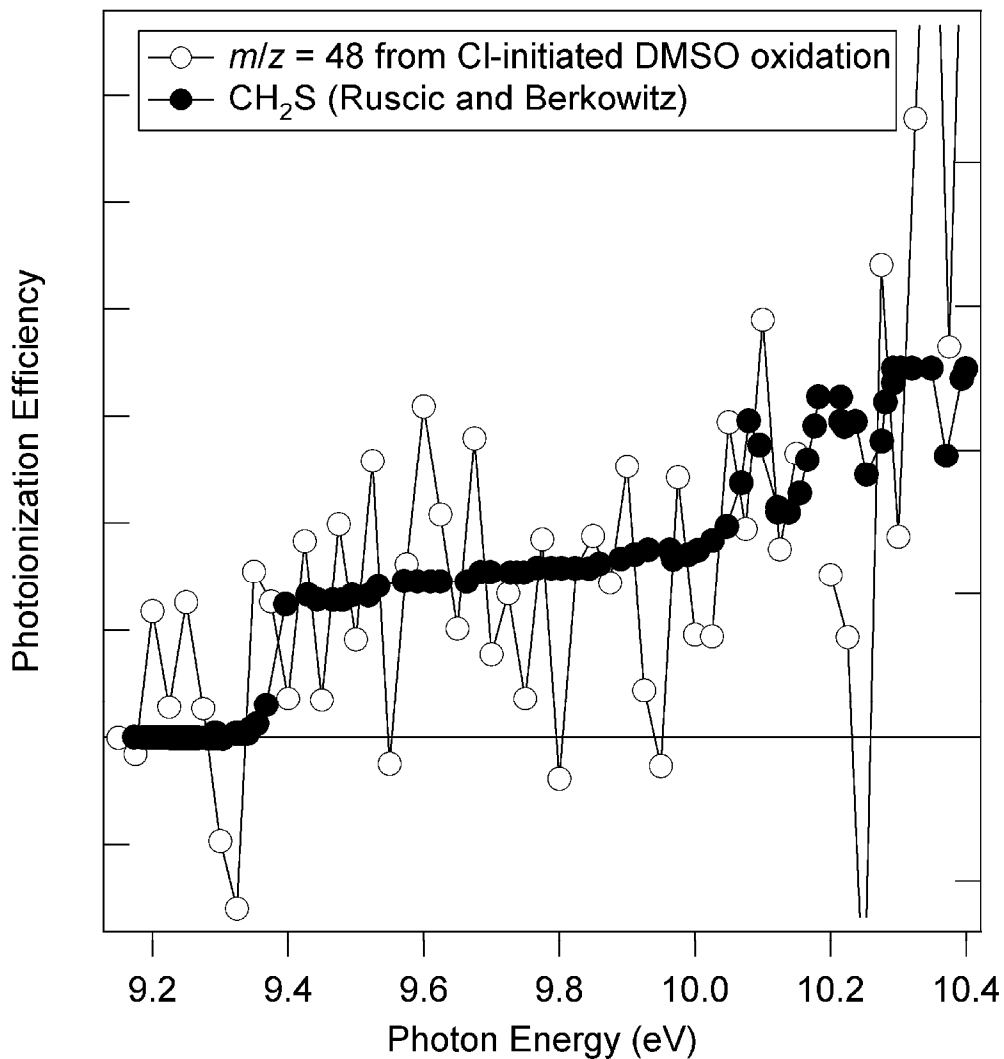


Figure S9. Photoionization efficiency spectrum of  $m/z = 48$  ( $\text{CH}_2^{34}\text{S}^+$ ) from the Cl-initiated DMSO oxidation, taken from the same experiment as the Criegee intermediate spectrum shown in the main paper. The spectrum is compared to the photoionization spectrum of thioformaldehyde ( $\text{CH}_2\text{S}$ )<sup>11</sup>. If the feature at  $m/z = 46$  that is attributed to  $\text{CH}_2\text{OO}$  were in fact due to production of  $\text{CH}_2\text{S}^+$  by dissociative ionization, it would be observed in this spectrum; however, it is absent.

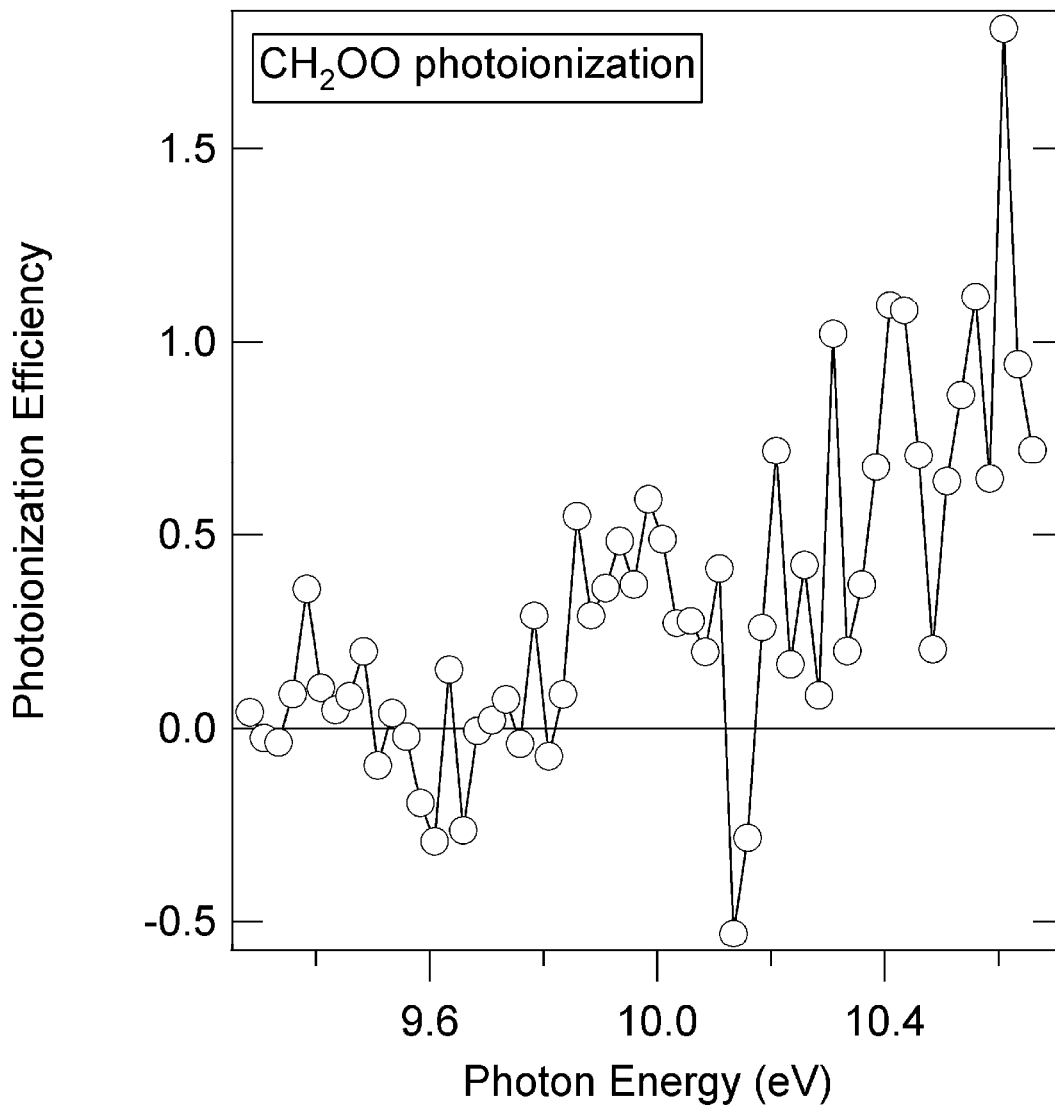


Figure S10. Low signal-to-noise photoionization spectrum attributed to the Criegee formaldehyde oxide, CH<sub>2</sub>OO, taken from experiments that suffered from more extensive dark chemistry than those shown in the main paper.

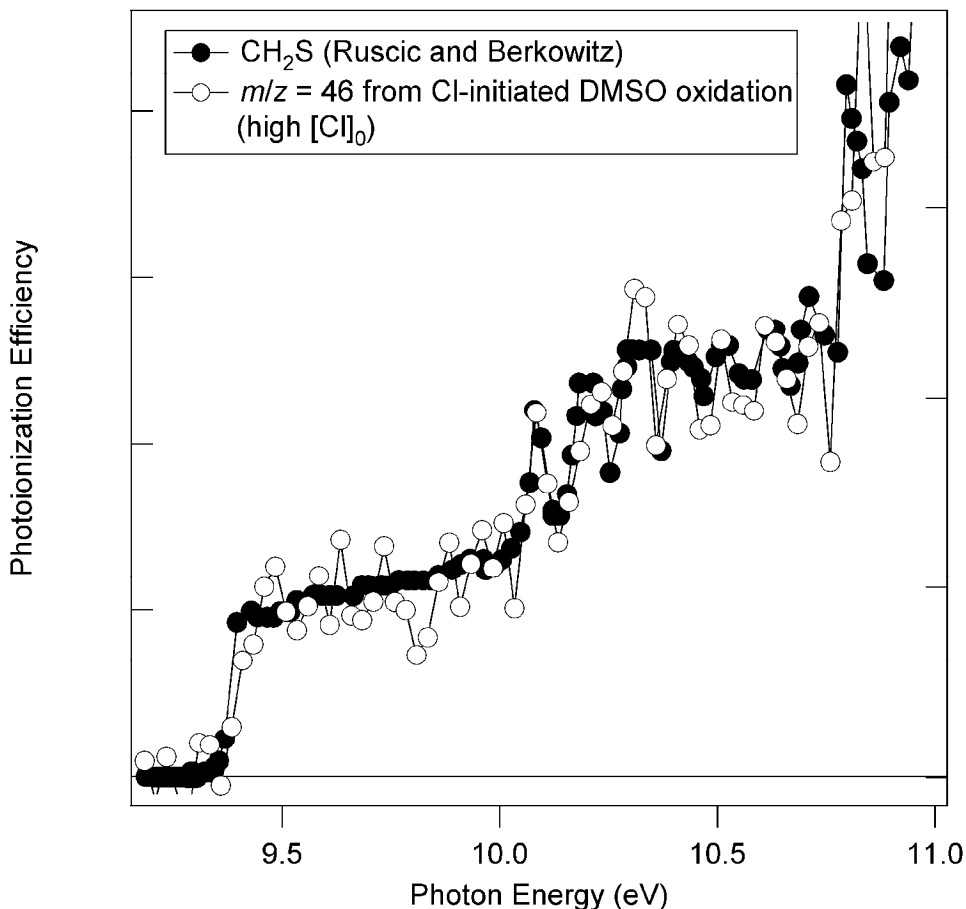


Figure S11. Photoionization efficiency spectrum of  $m/z = 46$  from Cl-initiated DMSO oxidation, taken with twice the  $(\text{ClCO})_2$  and one-fourth the DMSO of the experiments shown in the main paper. The spectrum is nearly identical to that of  $\text{CH}_2\text{S}^{11}$ ; the feature attributed to  $\text{CH}_2\text{OO}$  is absent (c.v. Figure 2 of the main paper), perhaps because of removal of  $\text{CH}_2\text{OO}$  or  $\text{CH}_3\text{SOCH}_2$  by excess Cl atom. The  $\text{CH}_3\text{SO}$  signal is also considerably reduced under these conditions relative to those in the experiments that showed  $\text{CH}_2\text{OO}$ . However, the concentrations of the most plausible sources of  $\text{CH}_2\text{S}^+$  by dissociative ionization, such as  $\text{CH}_3\text{SCl}$ , are similar.

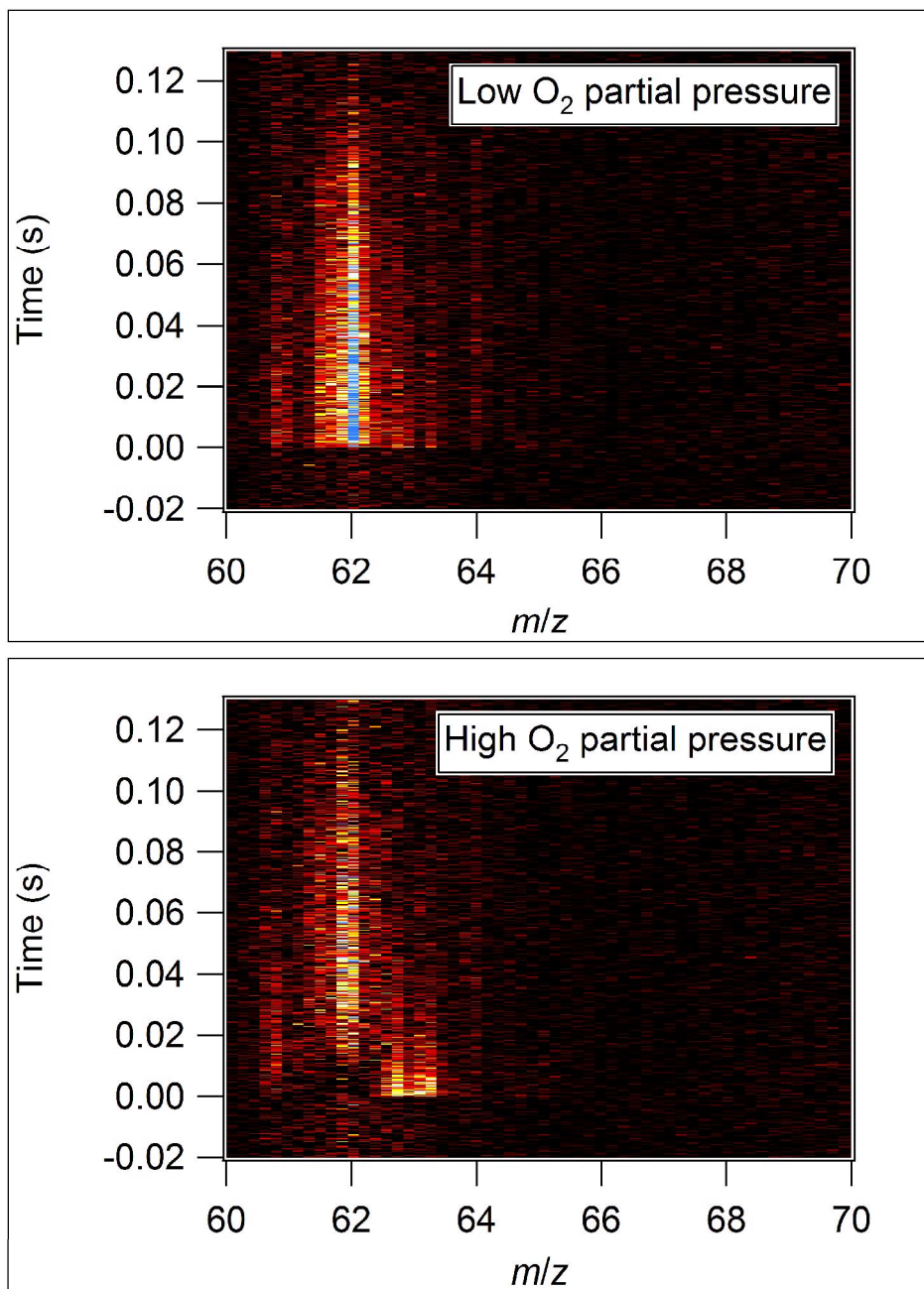


Figure S12. Dependence of the  $m/z = 62$  (dimethyl sulfide) and  $m/z = 63$  ( $\text{CH}_3\text{SO}$ ) signals on oxygen concentration. The  $\text{CH}_3\text{SO}$ , the coproduct of  $\text{CH}_2\text{OO}$  in the reaction of  $\text{CH}_3\text{SOCH}_2$  with  $\text{O}_2$ , is formed only in the presence of  $\text{O}_2$  (lower trace with  $\sim 2 \times 10^{16} \text{ cm}^{-3} \text{ O}_2$ ), and is largely absent at low  $\text{O}_2$  (upper trace with only residual  $\text{O}_2$  of  $\sim 10^{13} \text{ cm}^{-3}$ ).

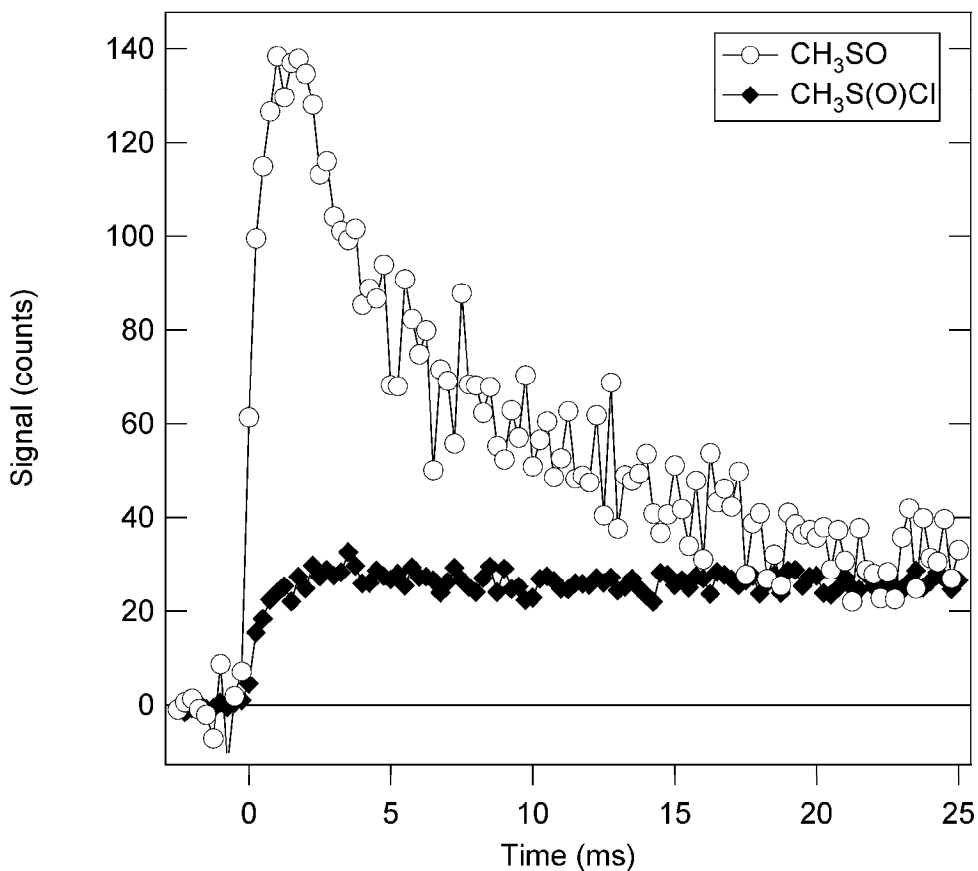
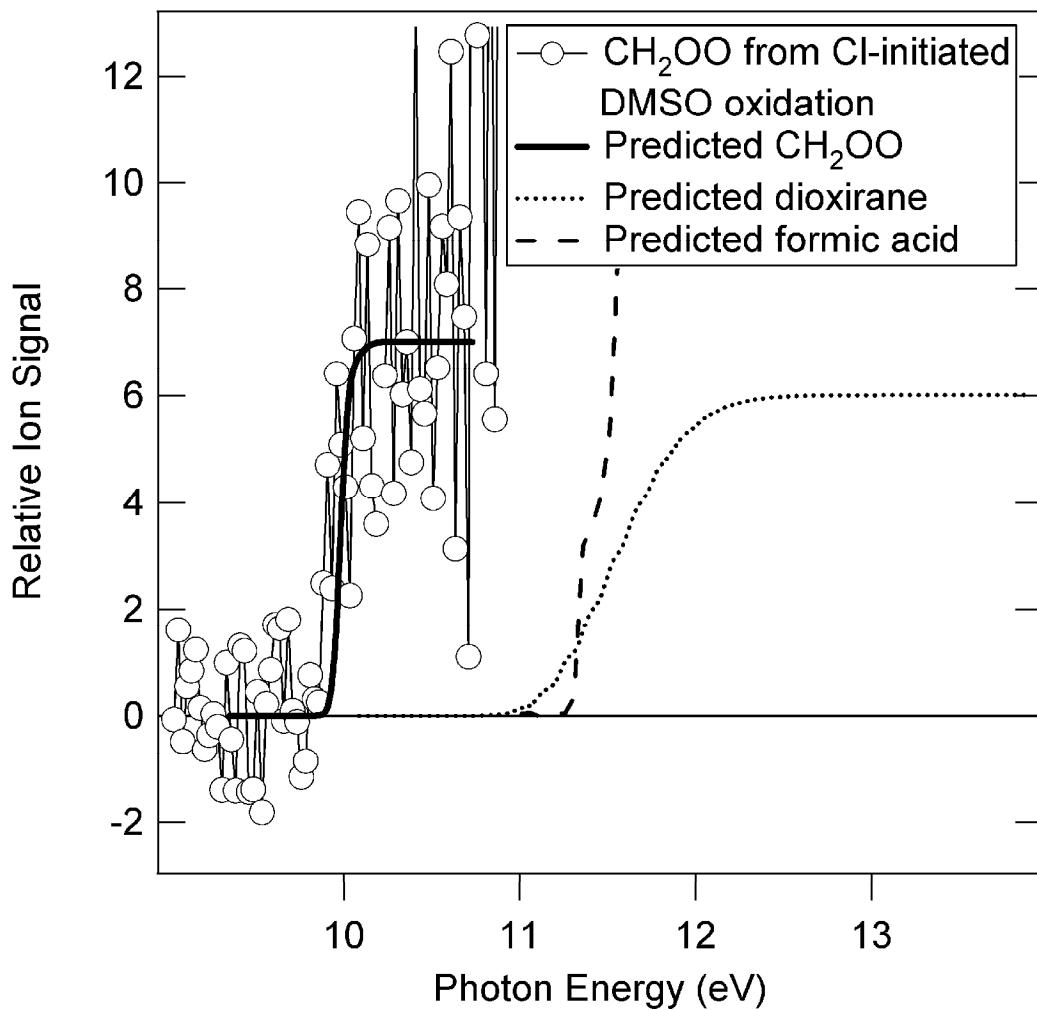


Figure S13. Comparison of the time behavior of CH<sub>3</sub>SO, the co-product of the Criegee intermediate CH<sub>2</sub>OO in the CH<sub>3</sub>SOCH<sub>2</sub> + O<sub>2</sub> reaction, with that of CH<sub>3</sub>S(O)Cl, a product of the Cl + DMSO reaction. The experimental conditions are as in Figure S1. The rate of production of CH<sub>3</sub>SO (and hence presumably CH<sub>2</sub>OO) is limited by the Cl + DMSO reaction.



**Figure S14.** Comparison of the measured CH<sub>2</sub>OO photoionization efficiency with the predicted photoionization efficiencies of the other CH<sub>2</sub>O<sub>2</sub> isomers.

Full references 7 and 22:

- (7) Guenther, A.; Hewitt, C. N.; Erickson, D.; Fall, R.; Geron, C.; Graedel, T.; Harley, P.; Klinger, L.; Lerdau, M.; McKay, W. A.; Pierce, T.; Scholes, B.; Steinbrecher, R.; Tallamraju, R.; Taylor, J.; Zimmerman, P. *J. Geophys. Res. Atmospheres* **1995**, *100*, 8873.
- (22) Frisch, M. J.; Trucks, G. W.; Schlegel, H. B.; Scuseria, G. E.; Robb, M. A.; Cheeseman, J. R.; Montgomery, J., J. A.; Vreven, T.; Kudin, K. N.; Burant, J. C.; Millam, J. M.; Iyengar, S. S.; Tomasi, J.; Barone, V.; Mennucci, B.; Cossi, M.; Scalmani, G.; Rega, N.; Petersson, G. A.; Nakatsuji, H.; Hada, M.; Ehara, M.; Toyota, K.; Fukuda, R.; Hasegawa, J.; Ishida, M.; Nakajima, T.; Honda, Y.; Kitao, O.; Nakai, H.; Klene, M.; Li, X.; Knox, J. E.; Hratchian, H. P.; Cross, J. B.; Bakken, V.; Adamo, C.; Jaramillo, J.; Gomperts, R.; Stratmann, R. E.; Yazyev, O.; Austin, A. J.; Cammi, R.; Pomelli, C.; Ochterski, J. W.; Ayala, P. Y.; Morokuma, K.; Voth, G. A.; Salvador, P.; Dannenberg, J. J.; Zakrzewski, V. G.; Dapprich, S.; Daniels, A. D.; Strain, M. C.; Farkas, O.; Malick, D. K.; Rabuck, A. D.; Raghavachari, K.; Foresman, J. B.; Ortiz, J. V.; Cui, Q.; Baboul, A. G.; Clifford, S.; Cioslowski, J.; Stefanov, B. B.; Liu, G.; Liashenko, A.; Piskorz, P.; Komaromi, I.; Martin, R. L.; Fox, D. J.; Keith, T.; Al-Laham, M. A.; Peng, C. Y.; Nanayakkara, A.; Challacombe, M.; Gill, P. M. W.; Johnson, B.; Chen, W.; Wong, M. W.; Gonzalez, C.; Pople, J. A. Gaussian 03; Revision C.02 ed.; Gaussian, Inc.: Wallingford, CT, 2004.

### References for Supplementary Material:

- (1) Meloni, G.; Selby, T. M.; Goulay, F.; Leone, S. R.; Osborn, D. L.; Taatjes, C. A. *J. Am. Chem. Soc.* **2007**, *129*, 14019.
- (2) Taatjes, C. A.; Hansen, N.; Osborn, D. L.; Kohse-Höinghaus, K.; Cool, T. A.; Westmoreland, P. R. *Phys. Chem. Chem. Phys.* **2008**, *10*, 20.
- (3) Meloni, G.; Zou, P.; Klippenstein, S. J.; Ahmed, M.; Leone, S. R.; Taatjes, C. A.; Osborn, D. L. *J. Am. Chem. Soc.* **2006**, *128*, 13559.
- (4) Ruscic, B.; Berkowitz, J. *J. Chem. Phys.* **1992**, *97*, 1818.
- (5) Hung, W.-C.; Shen, M.-y.; Lee, Y.-P.; Wang, N.-S.; Cheng, B.-M. *J. Chem. Phys.* **1996**, *105*, 7402.
- (6) Cheng, B.-M.; Chew, E. P.; Liu, C.-P.; Yu, J.-S. K.; Yu, C.-h. *J. Chem. Phys.* **1999**, *110*, 4757.
- (7) Nourbakhsh, S.; Notwood, K.; Yin, H.-M.; Liao, C.-L.; Ng, C. Y. *J. Chem. Phys.* **1991**, *95*, 946.
- (8) Cheng, B.-M.; Chew, E. P.; Yu, J.-S. K.; Yu, C.-h. *J. Chem. Phys.* **2001**, *114*, 4817.
- (9) Solouki, B.; Bock, H.; Appel, R. *Angew. Chem. Internat. Edit.* **1972**, *11*, 927.
- (10) Li, W.-K.; Chiu, S.-W.; Ma, Z.-X.; Liao, C.-L.; Ng, C. Y. *J. Chem. Phys.* **1993**, *99*, 8440.
- (11) Ruscic, B.; Berkowitz, J. *J. Chem. Phys.* **1993**, *98*, 2568.